

# Hydrogels from Polysaccharides. I. Cellulose Beads for Chromatographic Support

WILLER DE OLIVEIRA and WOLFGANG G. GLASSER\*

Biobased Materials Center, and Department of Wood Science and Forest Products, Virginia Polytechnic Institute and State University, Blacksburg, Virginia 24061-0323

## SYNOPSIS

Cellulosic hydrogels in bead form were prepared by dropwise addition of cellulose solutions in *N,N*-dimethylacetamide (DMAc) and lithium chloride (LiCl) to azeotropic methanol or isopropanol as nonsolvent. Bead properties were examined in relation to cellulose solution concentration, viscosity, and molecular weight. Bead properties were defined in terms of solids content, flow characteristics, mechanical strength, bead size, and pore dimensions. Results suggest that (a) beads can be prepared with solids content ranging from 2 to 12 wt %, depending on solution concentration; (b) uniform spherical shapes require a viscosity range between 100 and 300 cS; (c) beads can be produced in different sizes, within the diameter range of 100 to 1,500  $\mu\text{m}$ ; (d) linear flow velocities of packed bead columns are in the range of 70 to 350 cm/min; and (e) pore sizes of beads vary between 8 to 200  $\text{\AA}$ . Beads with low cellulose concentration show a wide fractionation range of up to 200,000 g/mol for polyethylene oxide. © 1996 John Wiley & Sons, Inc.

## INTRODUCTION

Purification and recovery of recombinant protein products can account for as much as 80% of total manufacturing costs for the biopharmaceutical industry.<sup>1,2</sup> Because most isolation and purification involves large-scale liquid chromatography, the availability of cost effective and efficient chromatographic support materials is of critical importance for advancements in bioprocessing technology. A general consensus for an ideal matrix is that it should exhibit the following requirements: high specificity (implying a surface charge content approaching zero); absence of hydrophobic binding sites; good chemical stability; good mechanical rigidity; high binding capacity; good recoverability; high reproducibility; and low cost.<sup>3-5</sup>

Hydrophilic polymers such as agarose and dextran have traditionally been used as supports for chromatographic procedures in biosciences and biotechnology.<sup>6,7</sup> During the early days of chromatog-

raphy, microcrystalline cellulose was used in powder form; however, this was found to be limited by poor flow characteristics and high pressure drops during column operation.<sup>8</sup> Since then, several techniques have been developed to replace the powder form by a more adequate particle shape, especially that of the spherical bead.<sup>9-11</sup> According to Stamberg,<sup>11</sup> spherical cellulose beads have been produced by a variety of processes, all having in common the following steps: (a) solvation of cellulose or cellulose derivative; (b) formation of a spherical droplet from the solution; (c) stabilization of the droplet; (d) phase inversion of the droplet so as to produce a gel; and (e) washing.

The major problem facing bead production was a lack of neutral cellulose solvents. Cellulose insolubility was overcome by using cellulose derivatives, such as cellulose acetate or xanthate (i.e., viscose), as starting material. The advent of novel solvent systems, such as DMAc/LiCl for cellulose, allowed the exploration of hydrogel production from unsubstituted cellulose.<sup>12,13</sup> This made it possible to take advantage of the exceptional rigidity of the cellulose backbone, which is the primary basis for hydrogel strength.

\* To whom correspondence should be addressed.

Cellulosic hydrogels in bead form have long been recognized for their superior strength properties under dynamic flow conditions. However, it was only recently that a rigorous and fundamental understanding of the interrelationship between pressure drop, flow velocity, solids content, and pore dimensions began to surface.<sup>14</sup>

In a study of the material aspects of beaded cellulosic hydrogels, Kaster et al.<sup>14</sup> introduced a design model for hydrogel-based immunosorbents that sought to optimize intraparticle protein transport, physical strength, pressure-flow characteristics, and dynamic capacity by manipulating bead size and solids content. Cellulose beads with solids contents of greater than about 9% dramatically reduced the permeability of large proteins such as thyroglobulin and beta-amylase into the gel matrix. Additionally, the amount of permeation by thyroglobulin at 3% bead solids content was about 10-fold larger than predicted by conventional diffusion models. A 1,000  $\mu\text{m}$  diameter beaded cellulose immunosorbent having 3% solids content gave equivalent capacity to a 140  $\mu\text{m}$  diameter beaded, crosslinked agarose support containing 4% solids. The authors concluded that the rapid intraparticle transport of large proteins in the 3% cellulose beads was evidence for an intraparticle transport regime symptomatic of both convection and diffusion.<sup>14</sup>

It was, therefore, the objective of the present study to examine production, flow, and separation capabilities of cellulosic hydrogels using the novel DMAc/LiCl solvent system in relation to polymer and materials characteristics.

## EXPERIMENTAL

### Cellulose Sources

Cellulose samples from different sources and representative of a large molecular weight range were used in this study. Cellulose powder ( $\text{DP}_n$  200 and  $\text{DP}_w$  300) was obtained from Whatman Paper Ltd. (CF-11); cellulose powder ( $\text{DP}_n$  100 and  $\text{DP}_w$  300) was obtained from Aldrich Chemical Company; chemical-grade wood pulp with  $\text{DP}_n$  averages of 900 ( $\text{DP}_w$  2500), 1200 ( $\text{DP}_w$  3000), 1400 ( $\text{DP}_w$  5300), and cotton linters with  $\text{DP}_n$  2100 ( $\text{DP}_w$  4000) were obtained from Eastman Chemical Company, Kingsport, TN. Cellulose samples were carbanilated, then dissolved in THF, and analyzed by gel permeation chromatography with a differential viscosity detector (Viscotek Model No. 100) and a differential re-

fractive index (concentration) detector (Waters 410) in sequence. All the calculations were based on a universal calibration curve.

### Solvents

*N,N*-Dimethylacetamide (DMAc) reagent grade was obtained from Fisher Scientific. Methyl and isopropyl alcohols were purchased from Baxter Scientific Products, and used without further purification.

### Others

Polyethylene oxide (PEO) and polyethylene glycol (PEG) were used as polymer probes, and they were procured from both Aldrich Chemical and Scientific Polymer Products, respectively. Lithium chloride (LiCl) certified grade was obtained from Fisher Scientific.

### Cellulose Dissolution

The dissolution of cellulose was based on the procedure of McCormick and Lichatowich.<sup>12</sup> Cellulose samples were solvent exchanged in DMAc for at least a week. Excess solvent was removed by filtration, and the dry weight was determined. The "activated" cellulose was stored for use. To dissolve cellulose, first a weighed amount of LiCl (8–10%, w/v) was dissolved in DMAc at 80°C. After complete dissolution of LiCl, a weighed amount of "activated" cellulose was added under continuous stirring. The mixture was kept at 80°C for 1 h, before it was cooled to room temperature with stirring continuing for 1–15 h or until complete dissolution was achieved.<sup>15</sup> Cellulose solution concentration varied from 0.5 to 8%, w/v.

### Beading Process

A solution of cellulose was atomized to form droplets using the apparatus shown schematically in Figure 1. Two nozzle types, with single and with multiple tips, were used. The former was able to handle small volumes (100–200 mL) of solution, and the latter could process up to 4 L per batch. In both cases, the cellulose solution was transferred from the solvent reservoir to the nozzle by applying pressurized nitrogen. The solutions were atomized into droplets by means of pressurized air jets pointed at the tip of the needle from which the solution protruded. The droplets were collected in a beaker containing

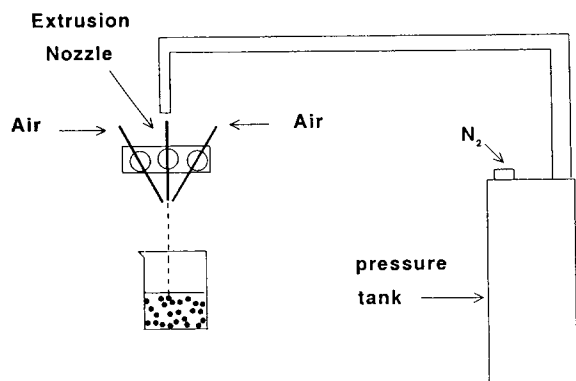


**Figure 1** Schematic representation of the instrumental beading setup. Bead formation is related to solution viscosity and air velocity as described by Su et al.<sup>16</sup>

isopropanol/water (azeotropic mixture, 8.8 : 1.2), or methanol/water after traveling several inches through open air. Solvent phase inversion was instantaneous, and the beads retained their spherical droplet shape.

DMAc/LiCl were removed first by washing with alcohol (isopropanol or methanol), and secondly by exhaustive water washing. The beads were kept in water and stored in a refrigerator.

### Pressure Drop Measurements

The mechanical strength of the beads was measured using a chromatographic column (Pharmacia, C 16/40, 16 mm × 40 cm), linked to an IBM-PC that controlled the pump speed and read the pressure from a pressure transducer (Fig. 2). Degassed water was pumped continuously from a reservoir through a 7 μm filter, a pulse dampener, the column, and a flow meter. A pressure transducer at the inlet of the column measured the change in pressure across the column bed. Water flowed upstream through the bead column, then through a flowmeter and back to the reservoir. Flow was programmed to increase continuously by less than 0.2 mL/min. An experiment was performed on dextran (Sephadex) beads and used as control. The results were presented in a plot of pressure drop, as given by

$$\text{Pressure drop [psi cm}^{-1}\text{]} = \frac{\text{Pressure [psi]}}{\text{column height [cm]}} \quad (1)$$

vs. linear velocity, expressed as

$$\text{Linear velocity [cm min}^{-1}\text{]} = \frac{\text{Flow rate [mL/min]}}{\text{column cross-section [cm}^2\text{]}} \quad (2)$$

### Solution Viscosity

The intrinsic viscosities of the cellulose solutions and the polymer probes were determined using a Cannon-Ubbelohde type of viscometer. All measurements were made in DMAc/LiCl solvent system at 22°C for the kinematic viscosity, and at 25°C for the intrinsic viscosity. The intrinsic viscosities, as well as the molecular weights and molecular diameters of equivalent spheres of the polymer probes used are given in Table I.

### Solids Content

The dry weight of the “activated” cellulose was calculated after methanol Soxhlet extraction of DMAc and drying the sample in a vacuum oven at 60°C until constant weight was achieved. The cellulose content of the beads was determined by either lyophilization or thermogravimetric analysis.

### Bead Size Distribution

Bead size distributions were determined using a computer imaging system that included a Carl Zeiss

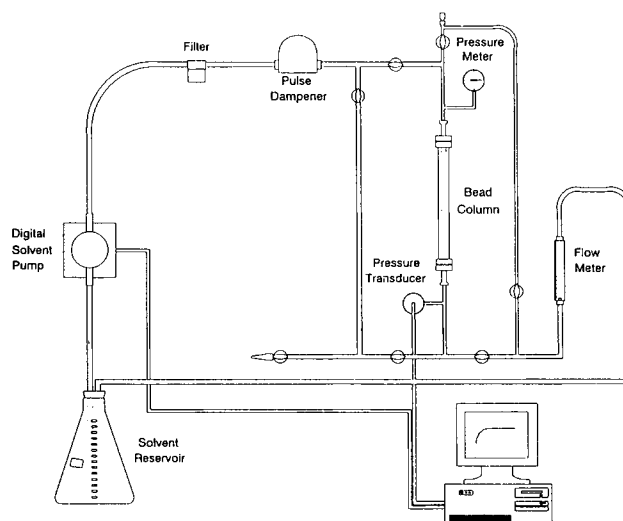


**Figure 2** Schematic representation of the instrumental setup for measuring pressure drop and crush velocity. The apparatus is programmed for dynamic flow rate variation and continuous pressure drop measurements.

**Table I** Molecular Weights, Intrinsic Viscosities, and Molecular Diameters of Equivalent Spheres of the Polymer Probes Used

| Polymer  | Molecular Weight, $M_w$ | MWD  | [IV] ( $\text{cm}^3/\text{g}$ ) | Molecular Diameter ( $\text{\AA}$ ) |
|----------|-------------------------|------|---------------------------------|-------------------------------------|
| PEO-300  | 305,400                 | 1.08 | 176.7                           | 403.2                               |
| PEO-200  | 200,000                 | —    | 128.1                           | 318.4                               |
| PEO-95   | 95,700                  | 1.02 | 104.5                           | 231.8                               |
| PEO-67   | 67,000                  | —    | 72.5                            | 178.2                               |
| PEG-20   | 20,000                  | —    | 33.5                            | —                                   |
| PEG-17   | 19,700                  | 1.34 | 29.6                            | 86.2                                |
| PEG-15   | 15,000                  | 1.2  | 25.5                            | 78.4                                |
| PEG-11   | 10,900                  | 1.18 | 18.0                            | 61.1                                |
| PEG-9    | 9,000                   | 1.1  | 20.1                            | 61.1                                |
| PEG-6.8  | 6,800                   | —    | 18.8                            | 54.4                                |
| PEG-5    | 5,000                   | 1.03 | 10.3                            | 40.2                                |
| PEG-3    | 3,070                   | 1.06 | 11.7                            | 35.3                                |
| PEG-1.5  | 1,490                   | 1.05 | 5.0                             | 21.0                                |
| PEG-0.6  | 629                     | 1.1  | —                               | 12.0                                |
| Methanol | 32                      | 1.0  | —                               | 3.1                                 |

Axioskop, and a DAGE MTI CCD-72 video camera linked to a PC fitted with an Image 1 A/T digital image analysis program. Each sample contained more than 100 beads taken randomly from a sample. The mean diameter of the beads was measured, and the standard deviation was calculated.

### Pore Size Analysis

The pore sizes of the beads were analyzed by gel permeation chromatography (GPC). This was performed using a Waters solvent delivery system with a Waters Model 650 sample injector. The column was from Pharmacia (C10/40, 10 mm  $\times$  40 cm). Column effluents were monitored by an Erma 7512 refractive index detector. The separation system is schematically illustrated in Figure 3. The cellulose beads were packed into the column forming a bed volume of 32 mL. The column was operated at constant speeds of 0.3, 0.5, and 1.0 mL/min. The following equation was used to calculate the chromatographic distribution coefficient,  $K_D$ ,

$$K_D = \frac{V_e - V_{e, \min}}{V_{e, \max} - V_{e, \min}} \quad (3)$$

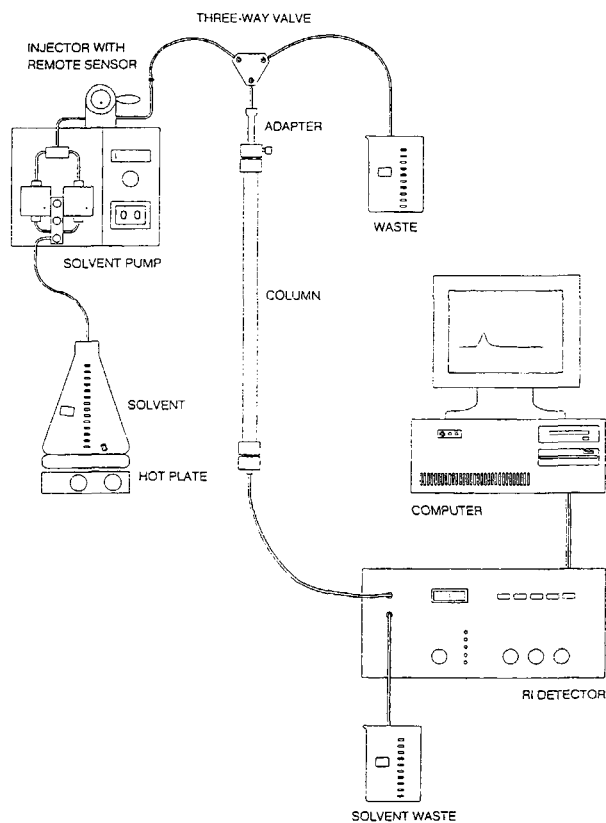
where  $V_e$  is the elution volume;  $V_{e, \min}$ , the elution volume of a totally excluded sample; and  $V_{e, \max}$  is the elution volume of a totally permeating sample.  $K_D$  is related to the elution volume; it can have a

value between 0 and 1. The relationship between distribution coefficient and molecular weight was displayed as a plot of log MW vs.  $K_D$ . Because molecular weight is directly related to molecular radius for any polymer in a given solvent, the log MW vs.  $K_D$  curve was adapted to show the dependence of  $K_D$  upon molecular radius. Polyethylene oxide (PEO) and polyethylene glycol (PEG) were used as molecular weight standards for column calibration. Their molecular diameter in water was calculated from the expression

$$R_v = 0.54 (M[\eta])^{1/3} \quad (4)$$

where  $R_v$  is the radius of a hydrodynamically equivalent sphere based on solute viscosity;  $M$  is molecular weight, and  $[\eta]$  is the intrinsic viscosity. The molecular weights and sizes of the standards are given in Table I.

The pore volume distribution was obtained by differentiating the  $K_D$  curve

**Figure 3** Schematic representation of the instrumental setup for determining pore characteristics.

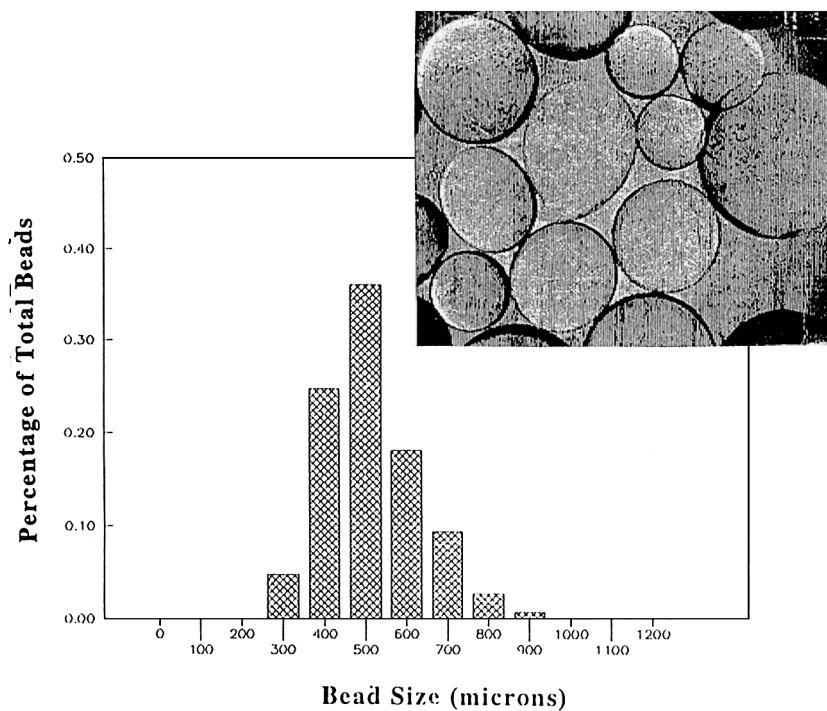


**Figure 4** Typical size distribution of cellulose beads as determined by image analysis. The bead sample shown in the inset had an average size of 467  $\mu\text{m}$ , with a standard deviation of 112 based on a sample size of 149 beads.

$$\text{Pore Volume} = \frac{(K_{D1} - K_{D2}) \Sigma_P}{(\log \phi_1 - \log \phi_2)} \quad (5)$$

where  $\phi_1$  and  $\phi_2$  are the molecular diameter of two consecutive standards; and  $\Sigma_P$  is the pore volume fraction.  $\Sigma_P$  was calculated by dividing the pore volume ( $V_P = V_{e,max} - V_{e,min}$ ) by the empty column volume.

## RESULTS AND DISCUSSIONS

### Formation

Conventional methodology for the formation of spherical polysaccharide hydrogels (“beads”) involves the dispersion of a polysaccharide solution in a medium of nonsolvent liquid phase. Bead size is thereby controlled by the creation of shear forces, and this involves efficiency of mixing during dispersion and the addition of surface active substances. In the present study, a solution extrusion method was adopted from Su et al. for sodium alginate solutions.<sup>16</sup> The breakup of the extruding fluid stream into spherical particles is thereby assisted by an air jet creating turbulence and shear at the

point of extrusion. This method of atomization is critical for cellulose solutions, which otherwise tend to form fibers. Parameters important for efficient droplet formation include viscosity, surface tension, and shear forces applied to the fluid stream. The transport of the fluid stream through turbulent air helps in the formation of spherical particles as shown in Figure 1. The droplets form an outer, permeable membrane following contact with a nonsolvent, such as aqueous methanol or isopropanol. Solvent exchange through this membrane (phase inversion) creates spherical gel particles, beads, with sizes that depend primarily on the dimensions of the atomizing nozzle. Cellulose beads were produced in a wide range of sizes, varying from 100 to 1,500  $\mu\text{m}$  in diameter, with a skewed distribution for a target average size. A typical size distribution of cellulose hydrogel beads (Fig. 4) reveals a more (in case of single tip nozzles) or less (in case of multiple tip nozzles) uniform distribution of 500  $\mu\text{m}$  size with a standard deviation of 100  $\mu\text{m}$ . The solids content of the water-washed, ash-free beads is related to both the solution concentration of cellulose (Fig. 5) and the composition of the nonsolvent (Fig. 6). Owing to the speed of phase inversion, no density gradient is expected to exist within the large hydrogel beads. In general

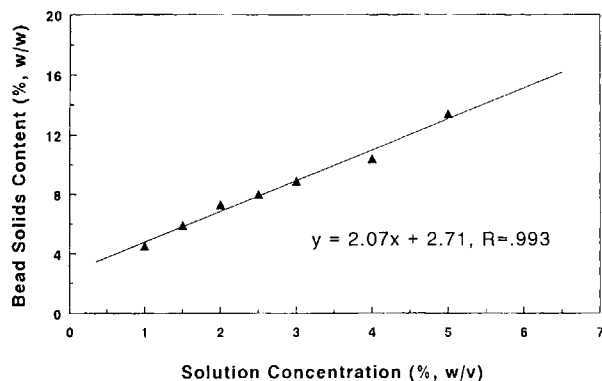


**Figure 5** Relationship between bead solids content and cellulose solution concentration.

it is possible to predict the final cellulose content in the beads through a relationship (Fig. 5) observed between the concentration of the cellulose in the solution with the actual cellulose concentration in the final bead. The relationship varies with the nature of the nonsolvent used.

Although it is possible to solubilize cellulose in DMAc/LiCl in concentrations up to 15% by weight,<sup>13</sup> solution viscosities of greater than 700 cS become too high for successful bead making. In fact, viscosity is the primary parameter determining "beadability." The relationship between the highest solution concentration of cellulose and cellulose molecular weight allowing bead production (Fig. 7) reveals an upper solution viscosity limit beyond which cellulose extrudes as filament rather than as bead. For instance, with DP<sub>n</sub> 200-cellulose (CF-11;  $M_n$ , 90,000 daltons), it is possible to produce beads from solution concentrations of up to 5% by weight, whereas DP<sub>n</sub> 1,220-cellulose ( $M_n$ , 635,000 daltons) is hardly "beadable" at concentrations as low as 0.6%. Beads could only be produced at solution viscosities below 700 cS, regardless of molecular weight (Table II). Solution viscosities above 700 cS could not be handled for beadmaking in the apparatus used. Therefore, the term "beadability" defines the viscosity boundaries for beading. Although beads with extremely low solids content can be produced, their mechanical strength is poor. The lowest solution viscosity allowing bead production was found to be around 20 cS. In order to increase bead strength and bead solids content, cellulose of lower molecular weight must be used. Based on Figure 7, it is predicted that with cellulose of DP 100 solutions having a concentration of up to 10% by weight can be beaded. Such low DP celluloses are typically obtained by partial hydrolysis or by steam explosion.<sup>17</sup>

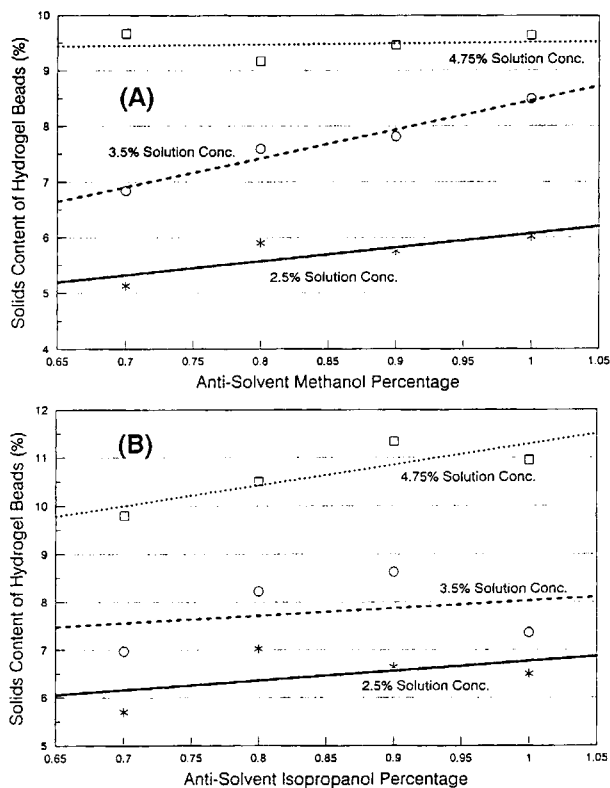


**Figure 6** Comparative cellulose bead characteristics using (A) methanol and (B) isopropanol-based nonsolvents. The balance of alcohol content is water.

In all cases, the preferred viscosity range for producing uniformly sized spherical beads is between 100 and 300 cS. Given constant solution viscosity and constant cellulose molecular weight, the process of bead generation is highly reproducible. Both bead

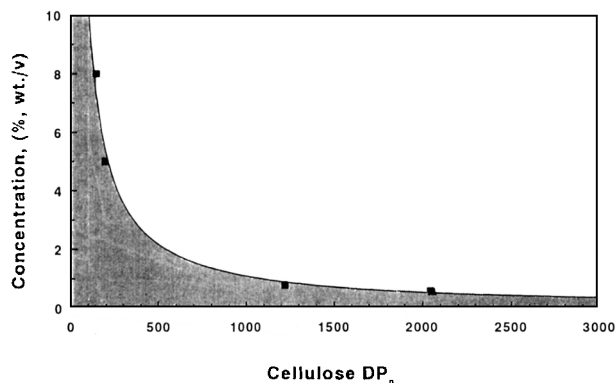


**Figure 7** Relationship between cellulose molecular weight and maximum allowable cellulose solution concentration for bead production. The area under the curve represents the region where beads can be made using the beading device shown in Figure 1.

**Table II Viscosity and "Beadability" of Cellulose Solutions**

|                                     | Viscosity<br>(cS) | Bead<br>Formation |
|-------------------------------------|-------------------|-------------------|
| Cellulose, $M_n = 89,300$           |                   |                   |
| Solution Concentration<br>(%, w/v)  |                   |                   |
| 5.5                                 | —                 | No                |
| 5.0                                 | —                 | No                |
| 4.0                                 | 479.2             | Yes               |
| 3.0                                 | 150.8             | Yes               |
| 2.0                                 | 34.1              | Yes               |
| 1.0                                 | 25.8              | Yes               |
| 0.5                                 | 15.7              | No                |
| Cellulose, $M_n = 634,800$          |                   |                   |
| Solution Concentration,<br>(%, w/v) |                   |                   |
| 0.80                                | 3670              | No                |
| 0.75                                | 2820              | No                |
| 0.70                                | 1800              | No                |
| 0.65                                | 1470              | No                |
| 0.60                                | 940               | No                |
| 0.55                                | 710               | Yes               |

size and bead solids content are highly predictable, and no uncontrollable differences in bead specifications have been noticed in more than 20 repetitions of bead making on the 1 to 4 L scale.

### Mechanical Strength

One of the most important properties of the cellulose beads is their mechanical strength, their ability to support fast flow of fluids without deformation, or without the development of high back pressures. The mechanical strength of cellulose beads in terms of the relationship between linear velocity and pressure drop reveals the pressure exponentiation behavior typical of hydrogels<sup>14</sup> (Fig. 8). The primary strength-determining variable is the solids content of the beads. Sephadex G-50 beads (source: Pharmacia LKB Biotechnology) were also analyzed under the same conditions for comparison. Flow rates as high as 350 cm/min can be sustained by cellulose beads without significant back pressure and without physical degradation. As a general rule, the higher the cellulose content of the hydrogels, the stronger the beads. In fact, beads with solids contents greater than 11% by weight failed to yield entirely to flow rates of 600 mL min<sup>-1</sup> (max. capacity of pump) corresponding to linear velocities of 300 cm min<sup>-1</sup>. On the other hand, Sephadex G-50 revealed the lowest

strength characteristics, about seven times lower than the cellulose beads with an equivalent solids content. In all the experiments, the bead size was greater than 350  $\mu\text{m}$  on average, one reason why Sephadex G-50 (300  $\mu\text{m}$ ) was selected for comparison.

The relationship between linear flow velocity and pressure drop across a 40 cm column reveals that most beads produce a nearly linear rise in linear velocity with pressure rising before pressure exponentiation is experienced (Fig. 8). The fact that the linear portion of the velocity vs. pressure drop relationship closely follows, without being identical, to theoretical expectations has been pointed out by Kaster et al.<sup>14</sup> (The deviation of experiment from theory, which suggests a faster rise of pressure drop as linear velocity increases, was attributed to particle deformation during flow).<sup>14</sup>

The second observation from the velocity vs. pressure drop relationship (Fig. 8), that of pressure exponentiation above a threshold flow velocity, indicates mechanical crushing of the chromatographic support. The relationship between crushing velocity (defined as the point where the flow rate crushes the beads) and bead solids content reveals an almost exponential rise with solids content (Fig. 9). The relationship between crushing velocity and bead diameter for cellulose beads with 4.8 and 8.9 % solids content, respectively, reveals linearity between crushing velocity and bead diameter (Fig. 10). In general, within a series with constant solids content, the higher the bead diameter, the higher the bead

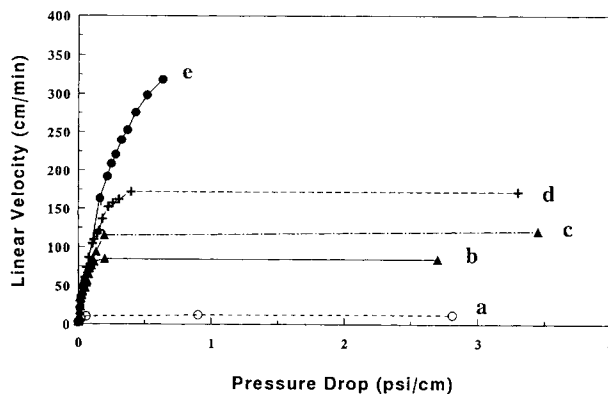


**Figure 8** Flow characteristics of cellulose beads (350  $\mu\text{m}$ ) in comparison with Sephadex G-50 (300  $\mu\text{m}$ ). The flow rates were determined on a column (40  $\times$  1.6 cm i.d., Pharmacia) with distilled water as mobile phase. Supports: (a) Sephadex G-50, (b–e) cellulose beads with increasing amounts of solids content: (b) 4.5%; (c) 5.9%; (d) 7.3%; and (e) 11.2%.

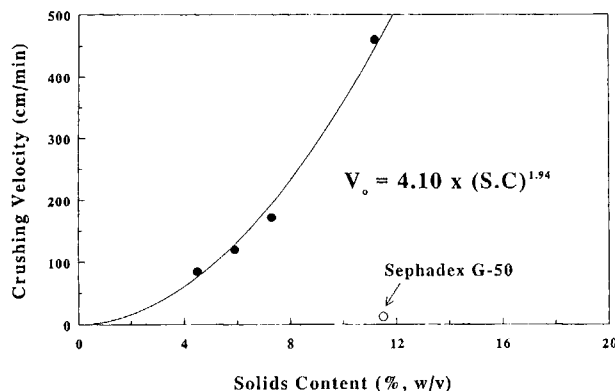


**Figure 9** Variation in the crushing velocity of cellulose beads as a function of cellulose solids content. Also shown in the figure is the crushing velocity of Sephadex G-50 with 11.5% solids content at comparable bead size.

strength. As the bead solids content doubles, its resistance to crushing also increases; and this effect is more dramatic for larger than for smaller beads. Figure 11, similarly to Figure 7, establishes the limits of bead strength achievable under current beading conditions. Surprisingly, this relationship implies that cellulose with the highest molecular weight produces the beads with the lowest strength. This is, of course, related to the concept of "beadability" defined above. Cellulose with high molecular weight is not "beadable" at elevated solution concentrations. Therefore, beads cannot be produced with higher solids content. The strongest beads are those made from solutions with highest cellulose content, and this requires celluloses of low molecular weight.

### Bead Morphology and Pore Size Distribution

The evaluation of bead morphology was attempted by scanning electron microscopy (SEM). Beads carefully dehydrated by (slow) freeze drying followed by desiccation in vacuum over  $P_2O_5$  exhibited SEM micrographs typical of hard glasses, without any sign of morphological differentiation. Attempts to gain insight into never-dried beads by environmental SEM failed on account of low solids content and insufficient distinctiveness of the carbohydrate molecules in water. Experiments with stained hydrated beads are currently underway using transmission electron microscopy. The results of these morphological studies by optical means will be reported in a forthcoming communication.

The measurement of bead porosity or pore volume distribution was performed by GPC. A typical chromatogram of a series of molecular probes on a cel-

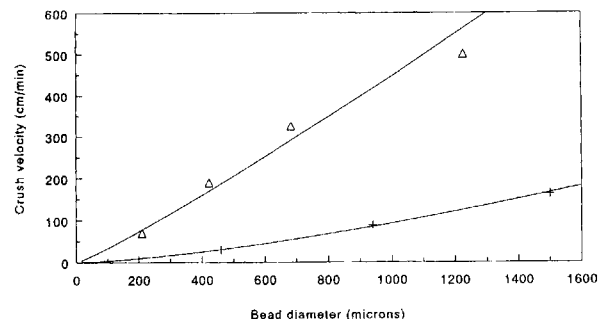


**Figure 10** Effect of size and solids content on flow characteristics of cellulose beads. Supports: cellulose beads with (+) 4.8% solids content; and (Δ) 8.9% solids content.

lulose bead column is shown in Figure 12. The peak on the top (i.e., PEO-300) represents the upper limit of separation, or  $V_{e,min}$ . The peak on the bottom (i.e., methanol) represents  $V_{e,max}$ , or the volume of a fully permeated molecule.

The complete molecular weight calibration curve and pore volume distribution (Fig. 13) was obtained by using several molecular probes of very low polydispersity. The interpretation of these curves can be regarded as the integral and the differential pore size distribution of a cellulose bead column. The  $K_D$  values are plotted against the logarithm of the molecular weight for different PEO and PEG standards. From the  $K_D$  curve (Fig. 13), the mean pore diameter can be determined chromatographically by taking the molecular diameter at  $K_D$  0.5. Figure 13 also shows the pore volume distribution obtained by taking the first derivative of the  $K_D$  curve. The results reveal pores capable of accommodating molecules sized between 10 and 1,000 Å following a uniform

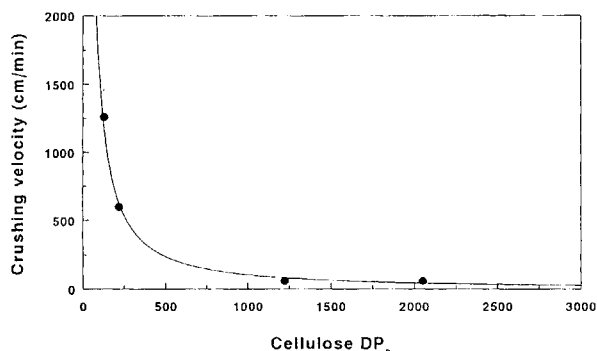


**Figure 11** Effect of cellulose molecular weight on flow characteristics of cellulose beads. The curve shows the predicted highest crushing velocities as a function of cellulose molecular weight for beads produced under the conditions described in the text.



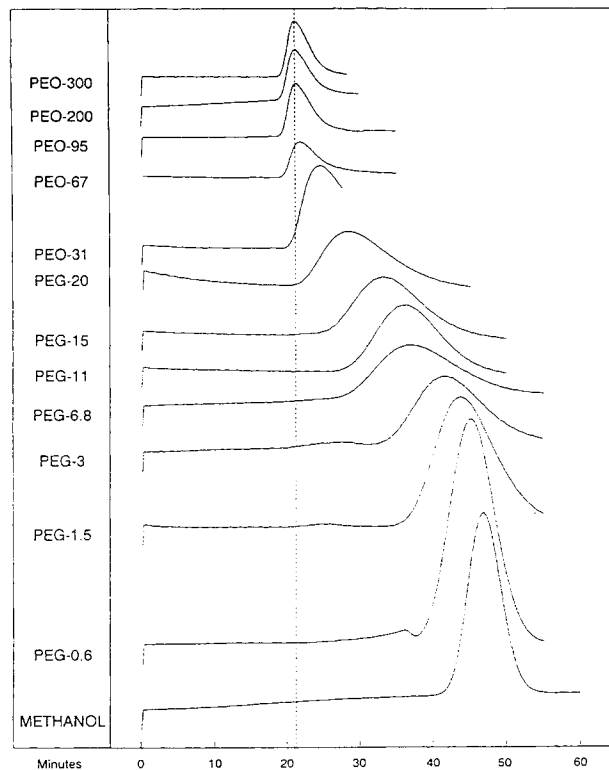


**Figure 12** Elution profile of methanol, polyethylene glycol (PEG), and polyethylene oxide (PEO) on 200 μm, 10.2% solids content cellulose beads. Chromatographic conditions: column dimensions: 32 × 1 cm; flow rate: 1 mL/min; and 20 μL sample volume.

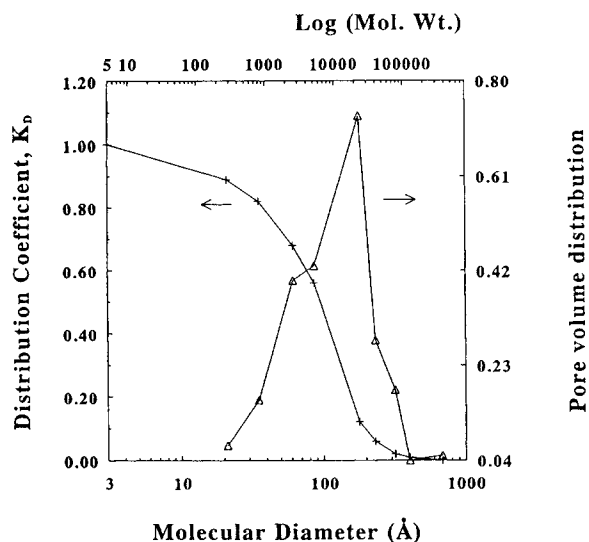


**Figure 13** Exclusion chromatographic calibration curve for cellulose beads with 5.1% solids content. The pore size distribution curve is obtained by differentiation of the calibration curve.

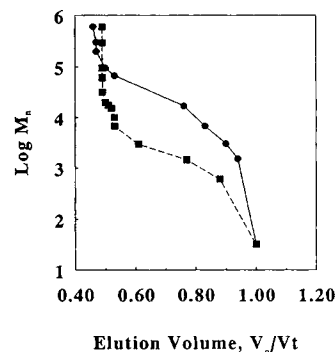


**Figure 14** Exclusion chromatographic calibration curves for cellulose beads with (●) 2.6%; and (■) 8.9% solids content.

distribution that peaks at 200 Å. The upper limit of the fractional range of this column for PEG was about 100,000 g/mol. Examples of calibration curves for beads with solids contents of 2.6 and 8.9% are shown in Figure 14. The higher the cellulose content, the smaller the pore size. Both the pore dimensions and the pore volume distribution vary with bead solids content, as illustrated in Figure 15.

Resolution capacity expressed as height equivalent to theoretical plates (HETP) is linearly related to linear flow velocity, and exponentially to particle diameter according to chromatographic theory.<sup>18</sup> Peak width at half height measurements of various molecular markers with respect to bead size and linear flow velocity reveal a deviation from expected behavior above a bead diameter of ca. 300 μm (Fig. 16). Similar results were reported by Regnier et al.<sup>19</sup> for perfusable sorbents, and by Kaster et al.<sup>14</sup> for ion exchange beads (DEAE-cellulose).

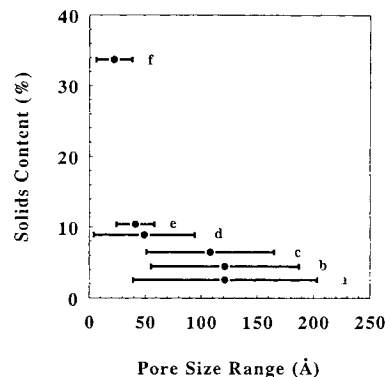


**Figure 15** Effect of bead solids content on pore size distribution. Supports: cellulose beads with increasing cellulose content: (a) 2.6%; (b) 4.5%; (c) 6.5%; (d) 8.9%; (e) 10.4%; and (f) 33.7%.

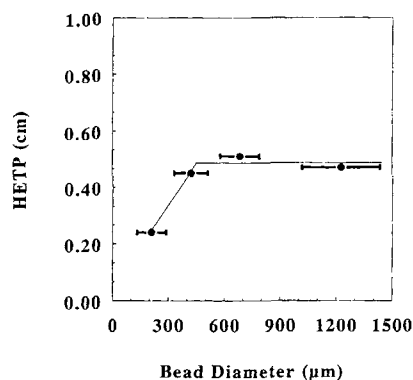


**Figure 16** Column resolution efficiency (expressed as height equivalent to theoretical plates) and bead diameter. The independence of HETP on size above 300  $\mu\text{m}$  indicates intraparticle convective transport.

### Transport Mechanism Considerations

Whereas convective flow favors the use of chromatographic particles with large diameter, resolution (e.g., height equivalent to theoretical plates, HETP) requires small particle dimensions and low linear flow velocity. Intraparticle, convective through-pore transport (e.g., "eddy diffusion," "perfusion") demonstrated that resolution capacity may remain independent of particle size and linear velocity. Using polystyrene-divinylbenzene as porous chromatographic support material with bimodal pore size distribution, Regnier et al. described beads with constant resolution capacity as bead diameter increased.<sup>19</sup> Such a behavior is observed also with cellulose beads of  $> 300 \mu\text{m}$  diameter (Fig. 16). Perfusion was achieved by the employment of diffusive pores having dimensions of 800 to 1,500  $\text{\AA}$  with a depth of  $> 10 \text{\AA}$ , and convective through-pores in the range of 6,000 to 8,000  $\text{\AA}$ .<sup>19</sup> Convective cellulose beads by contrast were found to have uniformly distributed pores ranging in size from 10 to 300  $\text{\AA}$  (Fig. 14). This observation supports the conclusion that intraparticle convective flow does not require bimodal pore distribution, but that this phenomenon can be observed as well with porous materials having uniform pore structure. It remains to be demonstrated whether the existence of two different pore geometries is required for achieving (dynamic) separation capacity. This will be the subject of a forthcoming study.

### CONCLUSIONS

1. Cellulose can be regenerated from DMAc/

LiCl-solution in the form of spherical hydrogel beads using azeotropic isopropanol or methanol as nonsolvent.

2. Bead solids content depends on solution concentration (primarily) and nonsolvent moisture content (secondarily).
3. Beadability in the particular instrument used (Fig. 1) is limited to solutions having a viscosity range between 30 and 700 cS. This impacts the range of useful cellulose molecular weights.
4. Flow behavior of cellulosic beads depends on solids content and diameter. Strength (crush resistance) increases with both solids content (almost exponentially) and size (linearly).
5. Celluloses with low DP, around 250, are required for beads with high strength. This is a consequence of both solution viscosity and bead solids content constraints.
6. Pore size distribution of cellulosic beads varies dramatically with bead solids content. Beads of  $< 3\%$  solids content have pores ranging from 50 to 200  $\text{\AA}$  in size, whereas beads with  $> 10\%$  solids content have pores in the range of 20–50  $\text{\AA}$ .
7. Resolution capacity is found not to depend on bead size for beads having diameters in excess of 300  $\mu\text{m}$ . This suggests intraparticle, convective through-pore transport reminiscent of perfusion.

The authors are indebted to Mr. Daniel Woodie for his skillful technical support in computer programming and execution of the pressure drop experiments. Thanks are also given to Mr. Paul McBee and Ms. Jody Jervis for carrying out the GPC analysis. This study was financially supported by a grant from the Center for Innovative Technology of Herndon, Virginia.

### REFERENCES

1. S. M. Wheelwright, *Bio/Technology*, **5**, 789 (1987).
2. C. H. Setchell, *J. Chem. Tech. Biotechnol.*, **35B**, 175 (1985).
3. Y. D. Clonis, *Biotechnology*, **7**, 1290 (1987).
4. E. V. Groman and M. Wilcheck, *Trends Biotechnol.*, **5**, 220 (1987).
5. S. R. Narayanan and L. J. Crane, *Tibtech*, **8**, 12 (1990).
6. J. Porath and P. Flodin, *Nature*, **183**, 1657 (1959).
7. J. Porath, J.-C. Janson, and T. Laas, *J. Chromatogr.*, **60**, 161 (1971).

8. Y. Motozato and C. Hirayama, *J. Chromatogr.*, **298**, 499 (1984).
9. J. Stamberg, J. Peska, D. Paul, and B. Philipp, *Acta Polym.*, **30**, 734 (1979).
10. J. Stamberg, J. Peska, H. Dautzenberg, and B. Philipp, in *Analytical Chemistry Symposia Series, Vol. 9, Affinity Chromatography and Related Techniques*, T. C. J. Gribnau, J. Visser, and R. J. F. Nivard, Eds., Elsevier, Amsterdam, 1982, p. 131.
11. J. Stamberg, *Sep. Purif. Methods*, **17**(2), 155 (1988).
12. C. L. McCormick and D. K. Lichatowich, *J. Polym. Sci., Polym. Lett. Ed.*, **17**, 479 (1979).
13. A. F. Turbak, A. El-Kafrawy, F. W. Snyder, and A. B. Auerbach, U.S. Pat. 4303252 (1982).
14. J. A. Kaster, W. de Oliveira, W. G. Glasser, and W. H. Velander, *J. Chromatogr.*, **648**, 79, (1993).
15. G. Samaranayake and W. G. Glasser, *Carbohydr. Polym.*, **22**, 1, 1993.
16. H. Su, R. Bajpai, and G. Preckshot, *Appl. Biochem. Biotechnol.*, **20/21**, 561 (1989).
17. S. C. Van Winkle and W. G. Glasser, *J. Pulp Paper Sci.*, **21**(2), J37-J43 (1995).
18. *Liquid Chromatography Terms and Relationships, ASTM E682*, American Society for Testing Materials, Philadelphia, 1979.
19. N. B. Afeyan, N. F. Gordon, I. Mazsaroff, L. Varady, S. P. Fulton, Y. B. Yang, and F. E. Ragnier *J. Chromatogr.*, **519**, 1-29 (1990).

Received July 14 1995

Accepted October 10 1995